Proc. Natl. Acad. Sci. USA
Vol. 91, pp. 10265–10269, October 1994
Biochemistry

Specific alteration of the oxidation potential of the electron donor in reaction centers from *Rhodobacter sphaeroides*

(bacteriochlorophyll/hydrogen bond/photosynthesis/purple bacteria/site-directed mutagenesis)

X. LIN†, H. A. MURCHISON†, V. NAGARAJAN‡, W. W. PARSON‡, J. P. ALLEN†§, AND J. C. WILLIAMS†§

†Department of Chemistry and Biochemistry, and Center for the Study of Early Events in Photosynthesis, Arizona State University, Tempe, AZ 85287-1604; and ‡Department of Biochemistry, SJ-70, University of Washington, Seattle, WA 98195

Communicated by Harry B. Gray, June 20, 1994

ABSTRACT **The effects of multiple changes in hydrogen bond interactions between the electron donor, a bacteriochlorophyll dimer, and histidine residues in the reaction center from *Rhodobacter sphaeroides* have been investigated. Site-directed mutations were designed to add or remove hydrogen bonds between the 2-acetyl groups of the dimer and histidine residues at the symmetry-related sites His-L168 and Phe-M197, and between the 9-keto groups and Leu-L131 and Leu-M160. The addition of a hydrogen bond was correlated with an increase in the dimer midpoint potential. Measurements on double and triple mutants showed that changes in the midpoint potential due to alterations at the individual sites were additive. Midpoint potentials ranging from 410 to 765 mV, compared with 505 mV for wild type, were achieved by various combinations of mutations. The optical absorption spectra of the reaction centers showed relatively minor changes in the position of the donor absorption band, indicating that the addition of hydrogen bonds to histidines primarily destabilized the oxidized state of the donor and had little effect on the excited state relative to the ground state. Despite the change in energy of the charge-separated states by up to 260 meV, the mutant reaction centers were still capable of electron transfer to the primary quinone. The increase in midpoint potential was correlated with an increase in the rate of charge recombination from the primary quinone, and a fit of these data using the Marcus equation indicated that the reorganization energy for this reaction is ≈400 meV higher than the change in free energy in wild type. The mutants were still capable of photosynthetic growth, although at reduced rates relative to the wild type. These results suggest a role for protein–cofactor interactions—in particular, histidine–donor interactions—in establishing the redox potentials needed for electron transfer in biological systems.**

Although the oxidation–reduction midpoint potentials of identical cofactors in redox proteins can vary by several hundred millivolts, the specific interactions of the cofactor with the protein that result in the variation in midpoint potential are not well understood. The primary electron donor in reaction centers from the purple photosynthetic bacterium *Rhodobacter sphaeroides* is a bacteriochlorophyll (Bchl) dimer designated P (reviewed in refs. 1–3). The two Bchls of the dimer, labeled A and B, overlap in ring I, where they are separated by ≈3.5 Å. The midpoint potential of the primary donor is ≈500 mV in wild-type reaction centers from *Rb. sphaeroides* (4–6) and is expected to be a critical parameter for electron transfer reactions that involve the donor, as alteration of the potential will result in a change in the driving force for these reactions.

Mutagenesis experiments have shown that hydrogen bonds between histidine residues and the conjugated carbonyls of the Bchls in the dimer can alter the midpoint potential by significant amounts (5, 7–10). For each Bchl there are two groups, the 9-keto group of ring V and the 2-acetyl group of ring I, that are part of the conjugated π electronic system and are possible proton acceptors for hydrogen bonds. Structural and spectroscopic data indicate that in the wild-type *Rb. sphaeroides*, these groups form only one hydrogen bond, between His-L168 and the acetyl group of the A-side Bchl (P_A) of the dimer (11–14). To characterize the effects of alterations in the hydrogen bonding patterns on the oxidation potential of the dimer, mutants have been constructed with changes near the four conjugated carbonyl positions (Fig. 1). The individual mutations are His to Phe at L168 [mutant HF(L168)], designed to remove the hydrogen bond to the 2-acetyl group of P_A; Phe to His at M197 [mutant FH(M197)], designed to add a hydrogen bond to the 2-acetyl group of P_B; and Leu to His at L131 [mutant LH(L131)] and Leu to His at M160 [mutant LH(M160)], designed to add a hydrogen bond to the 9-keto group of P_A and P_B, respectively. Fourier-transform infrared and resonance Raman spectroscopic data from reaction centers with these individual mutations and also a double mutant containing changes at both L131 and M160 confirm that the hydrogen bonding patterns are as expected (15, 16). Removal of the hydrogen bond by the mutation His to Phe at L168 decreases the oxidation potential by ≈80 mV, as measured by chemical redox titrations of isolated reaction centers (10), whereas the addition of a hydrogen bond to the 9-keto groups by the mutation Leu to His at L131 or Leu to His at M160 increases the oxidation potential by ≈80 or ≈60 mV, respectively (5). Preliminary results on a double mutant combining the changes at L131 and M160 indicate that the changes in potential are additive (9).

A complete set of all of the double mutants of these residues has now been constructed, as well as a triple mutant incorporating the three mutations that result in addition of a hydrogen bond, thus producing a reaction center presumed to have the maximum of four hydrogen bonds at these positions. We present a characterization of the effects of these mutations on the oxidation potential of the dimer, as well as an examination of the consequences of the altered potentials on some of the functional properties, including the rate of charge recombination between the primary electron donor (P^+) and the primary quinone acceptor (Q_A^-).

METHODS

Strain Construction and Protein Isolation. The double and triple mutants were constructed by oligonucleotide-directed mutagenesis and cloning of restriction fragments (5, 9, 10). The mutant FH(M197) in *Rb. sphaeroides* was created by

The publication costs of this article were defrayed in part by page charge payment. This article must therefore be hereby marked "*advertisement*" in accordance with 18 U.S.C. §1734 solely to indicate this fact.

Abbreviations: Bchl, bacteriochlorophyll; P, primary electron donor; Q_A, primary quinone acceptor.

§To whom reprint requests should be addressed.

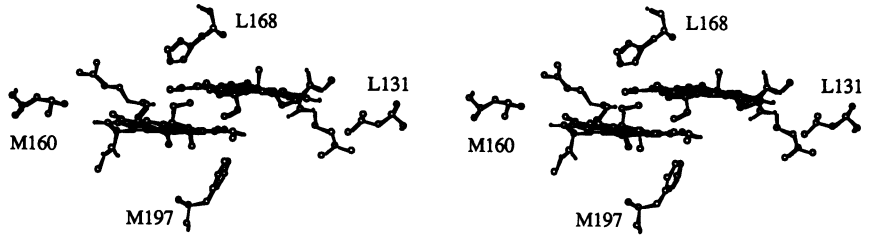

FIG. 1. Stereoview of the Bchl dimer and residues Leu-L131, His-L168, Leu-M160, and Phe-M197 of the reaction center from *Rb. sphaeroides*. The view is down the twofold symmetry axis of the dimer. Coordinates are from file 4RCR of the Brookhaven Protein Data Bank.

cassette mutagenesis, as described previously for the mutant *syml* in *Rhodobacter capsulatus* (7). The mutated genes were expressed in the *Rb. sphaeroides pufLM* deletion strain ΔLM1.1 (17). For all experiments, wild-type reaction centers were those isolated from the strain ΔLM1.1 complemented with a plasmid containing the wild-type genes. Cells were grown semiaerobically and reaction centers were isolated from all strains by published procedures (5, 17). The isolated reaction centers from all strains were pure, with an A_{280}/A_{800} ratio of <1.6, and did not degrade during the photooxidation studies.

Steady-State and Transient Optical Spectroscopy. Optical absorption spectra of isolated reaction centers were measured with a Cary 5 spectrophotometer (Varian) at 295 K. The rate of charge recombination between P^+ and Q_A^- was measured on a kinetic spectrophotometer of local design (18). A Surelight laser (Continuum) with a 5-ns pulse width was used for excitation of the sample at 532 nm. The time course of the change in absorption of the Q_y transition (860 nm for wild type) was measured on reaction-center samples ($A_{802}^{1\,cm} \approx 1$) in 15 mM Tris Cl, pH 8/1 mM EDTA/0.025% lauryldimethylamine *N*-oxide/0.5 mM terbutryn. Measurements were made at both 24°C and 8°C.

Oxidation–Reduction Titrations. The P/P^+ midpoint potential was determined by electrochemical oxidation–reduction titrations. The degree of reduction of the dimer was measured by monitoring the absorption at the maximum of the dimer Q_y absorption band (865 nm in the wild type) while recording the ambient redox potential. For the electrochemical titrations, the reaction centers were in 20 mM Tris Cl, pH 8/1 mM EDTA/0.1% Triton X-100/60 mM KCl, with 0.15 mM potassium tetracyanomono(1,10-phenanthroline)ferrate(II) tetrahydrate or 0.4 mM dicyanobis(1,10-phenanthroline)iron(II) dihydrate added as a mediator. The titrations were performed (6) in a thin-layer electrochemical cell similar to that described by Moss *et al.* (4). The data were fit to the one-electron Nernst equation:

$$\frac{[P]}{[P^+]} = \frac{A - A_{ox}}{A_{red} - A} = \exp[0.03894(E_m - E)], \qquad [1]$$

where E is the measured ambient potential, E_m is the midpoint potential, A is the absorbance of the dimer Q_y peak, A_{red} is the absorbance of a fully reduced sample, and A_{ox} is the absorbance of a fully oxidized sample. The data were fit with three free parameters, E_m, A_{red}, and A_{ox}.

Photosynthetic Growth. Aerobically grown cultures were diluted in the growth medium plus 0.8% agarose in spectrophotometric cuvettes and sealed. Photosynthetic growth was at ≈25°C with illumination from a tungsten source at a light intensity of ≈25 lx as measured with a model LI185B photometer (Li-Cor, Lincoln, NE). The growth rate was determined from the slope of a linear fit of ln A_{680} vs. time during the exponential portion of the growth.

RESULTS

Optical Absorption Spectra. Room-temperature (≈295 K) optical absorption spectra of the mutant reaction centers were similar to those of wild type, indicating that the structure of the protein is largely unchanged (data not shown). All mutants containing the L168 change showed blue shifts of 10–40 nm in the position of the Q_y band of the dimer, which is at ≈865 nm in the wild type. Thus, although the energy of the P/P* transition is essentially unchanged in most mutants, some differences are noted for the mutants with the loss of the hydrogen bond between P and His-L168. The spectral shifts could reflect rotation of the acetyl group or alteration of the overlap between the two Bchls. A more complete discussion concerning changes in the optical spectra and the spectral features of P^+ will be presented elsewhere (T. A. Mattioli, B. Robert, X.L., J.C.W., and J.P.A., unpublished work).

P/P^+ Oxidation Potential. The midpoint potential values reported for the electrochemical titrations are for fits of the combined oxidative and reductive data to the Nernst equation ($n = 1$), rounded to the nearest 5 mV (Table 1). An error of ±5 mV was estimated, based on the variation in different titrations of the wild type. For some of the electrochemical titrations, the amplitude of the fully reduced sample did not return to the original value, probably due to dilution of the sample [e.g., HF(L168) in Fig. 2]. However, this difference did not significantly affect the results, as the average difference between the oxidative and reductive titrations when fit separately was 5 mV. The average difference between the values for chemical titrations performed previously (5, 9, 10) and the electrochemical titrations was 7 mV, and generally the electrochemical titration value was higher. The slightly higher values for the electrochemical titrations probably were due in part to the higher ionic strength of the buffer, since a chemical titration of the wild type in the same buffer used for the electrochemical titrations yielded a midpoint potential that was ≈5 mV higher than that obtained in the usual buffer for chemical titrations.

The electrochemical titrations allowed nearly complete titrations to be obtained from all of the mutants (Fig. 2). A

Table 1. Comparison of P/P^+ midpoint potential and $P^+Q_A^- \rightarrow PQ_A$ charge recombination time for dimer hydrogen-bond mutants

Strain	No. of dimer hydrogen bonds	E_m, mV	ΔE_m, mV	τ, ms
HF(L168)	0	410	−95	220
HF(L168)/LH(M160)	1	485	−20 (−35)	110
LH(L131)/HF(L168)	1	485	−20 (−15)	175
Wild type	1	505		100
HF(L168)/FH(M197)	1	545	40 (30)	55
LH(M160)	2	565	60	75
LH(L131)	2	585	80	70
FH(M197)	2	630	125	65
LH(L131)/LH(M160)	3	635	130 (140)	60
LH(M160)/FH(M197)	3	700	195 (185)	45
LH(L131)/FH(M197)	3	710	205 (205)	55
LH(L131)/LH(M160)/FH(M197)	4	765	260 (265)	40

ΔE_m is the difference in the P/P^+ midpoint potential between the mutants and the wild type. For the strains containing multiple mutations, the number in parentheses is the sum of the changes found in the strains containing the individual mutations.

striking feature of the results is the additive nature of the changes in the midpoint potential. The change in midpoint potential for each multiple mutant is very similar to the sum of the changes observed for the corresponding single-site mutants (Table 1). Thus, the midpoint potential was lowered by 95 mV by the loss of the existing hydrogen bond and was increased by 60–125 mV for the addition of each hydrogen bond. Due to this additive effect, a very high midpoint potential of 765 mV, or 260 mV above wild type, was observed for the mutation that has three hydrogen bonds added.

$P^+Q_A^-$ Charge Recombination Rate. The kinetics of charge recombination between P^+ and Q_A^- were measured by the recovery of the bleaching of the Q_y band of P after excitation with a laser pulse in the presence of terbutryn. The extent of bleaching in the mutants was similar to that of wild type, indicating that electron transfer to the quinone occurs in all the mutants. Since saturating conditions were used, the amount of $P^+Q_A^-$ formation does not yield direct information concerning the quantum efficiency of charge separation. In general, an increase in the midpoint potential of the reaction centers was correlated with an increase in the charge recombination rate (Fig. 3; Table 1). The rate was independent of temperature from 24°C to 8°C within the error of the measurement (±5%).

Photosynthetic Growth. Photosynthetic growth was observed for all of the mutant strains, although the rate of growth was slower than for wild type. The mutants with midpoint potentials within 100 mV of wild type generally showed an ≈2-fold reduction in the photosynthetic growth rate. The mutants with the higher midpoint potentials had slower growth rates, up to an ≈10-fold reduction in rate for the triple mutant LH(L131)/LH(M160)/FH(M197), which had the highest midpoint potential.

DISCUSSION

An unusually large range, 350 mV, in the midpoint potential resulted from changes in the hydrogen bonding pattern between histidine residues and the Bchl dimer in reaction centers. This large range was achieved because the changes in midpoint potential resulting from single mutations were additive in reaction centers with multiple mutations. The additivity of multiple mutations indicates that the effects of the changes are local and that the sites have little electrostatic or structural interactions (reviewed in ref. 19). Despite these large changes in midpoint potential, the reaction centers were still functional in the sense that electrons could be transferred to Q_A, and all of the mutants were capable of photosynthetic growth. The introduction of a hydrogen bond between histidine and P appears to destabilize the oxidized state, P^+, relative to the ground state but has little effect on the energy of the excited state, P*, relative to the ground state (Fig. 4). It seems likely that the large changes in the oxidation potential arise from electrostatic interactions of P^+ with the histidine. In addition to the changes in the energy level, large changes in the electron distribution in P^+ due to the introduction of the histidine residues have been demonstrated by changes in the relative electron spin densities on the two halves of P^+ as measured by electron–nuclear double resonance and Fourier-transform resonance Raman spectroscopy (16, 20).

Due to the changes in the P/P^+ midpoint potential, the driving force for several electron transfer reactions will be altered, and so the relationship between the rate and driving

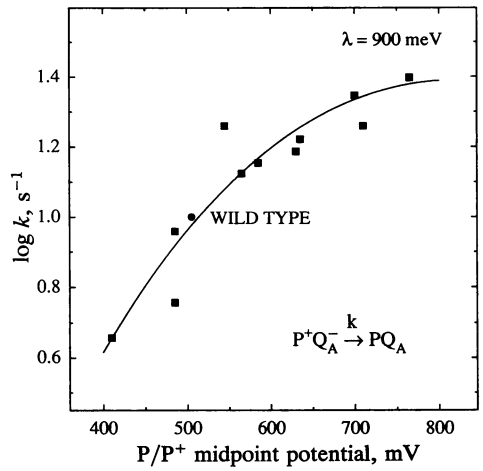

FIG. 3. The relationship between the charge recombination rate constant and the P/P^+ midpoint potential for wild type (●) and the hydrogen bond mutants (■). The curve results from a fit of Eq. 2 to the data with the parameters $V_{12} = 3.5 \times 10^{-9}$ eV, $\lambda = 900$ meV, and $\nu = 1240$ cm^{-1}.

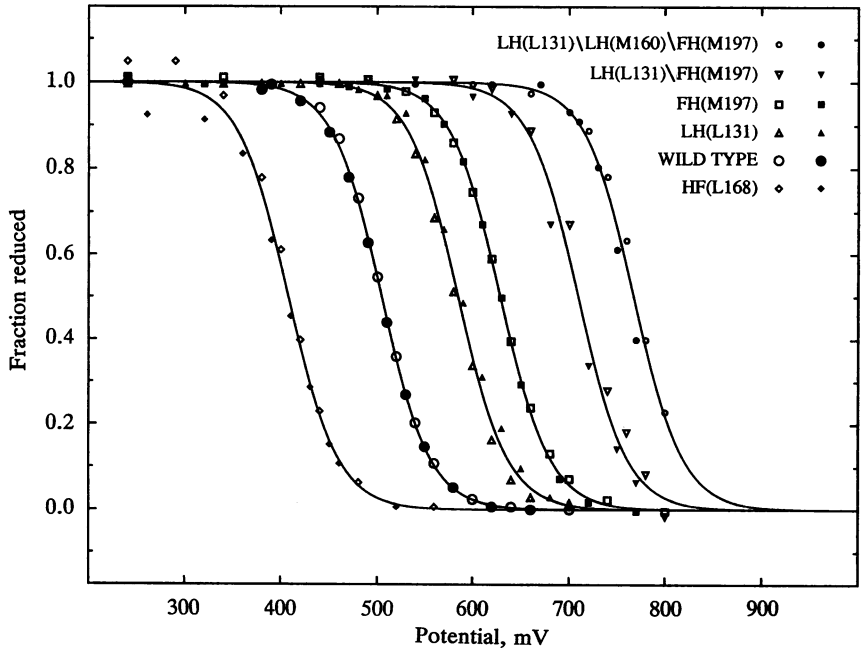

FIG. 2. Electrochemical oxidation–reduction titrations of reaction centers isolated from wild type and several hydrogen bond mutants. The extent of reduction was determined by monitoring the optical absorption of the donor band (at 865 nm in wild type) during the titration. The open symbols represent data from an oxidative titration and the filled symbols represent data from a subsequent reductive titration on the same sample. The lines represent fits of the combined data to the Nernst equation ($n = 1$). The midpoint potential values for all of the strains are summarized in Table 1.

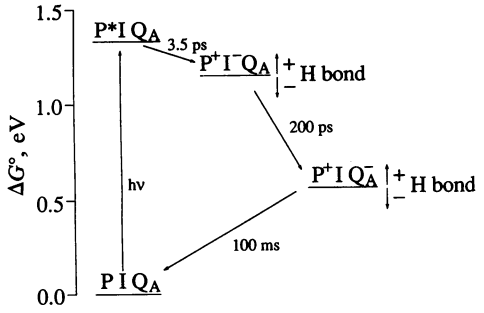

FIG. 4. Simplified free-energy diagram showing the relative effects of the mutations on the states in the reaction center involving P, the intermediate acceptor (I), and Q_A. The addition of a hydrogen bond to P causes an increase in the P/P^+ midpoint potential, and the removal of a bond causes a decrease in the potential. This results in corresponding changes in the energy levels of the charge-separated states involving the intermediate acceptor ($P^+I^-Q_A$) and the primary quinone acceptor ($P^+IQ_A^-$) but does not significantly alter the energy level of the excited state (P^*IQ_A) relative to the ground state (PIQ_A).

force can be studied. Examination of this relationship for charge recombination from the primary quinone allows testing of electron transfer models for a direct reaction and comparison with other experimental studies of this relationship. In a widely used general model that assumes that the donor and the acceptor are coupled to a single vibrational mode in a harmonic approximation (21), the rate is given by

$$k = \frac{4\pi^2}{h}\left(\frac{1}{h\nu}\right)|V_{12}|^2\left(\frac{v+1}{v}\right)^{p/2} \times \exp[-S(2v+1)]I_p\{2S[v(v+1)]^{1/2}\}, \quad [2]$$

where V_{12} is the electronic coupling matrix element; $v = 1/\{\exp[(h\nu/k_BT) - 1]\}$ and is the thermal population of a mode with vibrational frequency ν at temperature T, where k_B is the Boltzmann constant; $p = -\Delta G°/h\nu$; $I_p\{\ \}$ is a modified Bessel function of order p; and $S = \lambda/h\nu$, where λ is the reorganization energy (22). To fit the rate of the $P^+Q_A^-$ recombination reaction to this expression, a value for $\Delta G°$ of $\approx$0.50 eV for wild-type reaction centers (23) was used, and the changes in the P/P^+ midpoint potential in the mutants were assumed to cause parallel changes in $\Delta G°$. Changes in the Q/Q^- midpoint potential probably are negligible, because the quinone is relatively distant from the sites of the mutations. The data were well fit to Eq. 2 when the parameters were adjusted to the values $\lambda = 900$ meV and $\nu = 1240$ cm^{-1} (Fig. 3). While λ must be larger than 800 meV, the exact value or the possible contribution of additional vibrational modes cannot be determined from these data, since a maximum rate has not been clearly observed. The value for ν can be varied by ± 100 cm^{-1} without significantly affecting the quality of the fit. The data did not fit well to the classical Marcus expression (21), which predicts a steeper increase in rate with midpoint potential than is observed; the large value for ν obtained from Eq. 2 is consistent with this poor fit, since the corresponding characteristic temperature ($h\nu/k_B = 1800$ K) is much higher than the experimental temperature (295 K).

The fit of the charge recombination data to Eq. 2 assumes that charge recombination occurs by the same mechanism in the mutant and wild-type reaction centers. In the wild type the charge recombination reaction occurs by a direct, nonactivated process. When the midpoint potential of the quinone is shifted, recombination can occur by an indirect route through an intermediate electron carrier, I (24, 25). This indirect route probably is not important in the mutants, because it would result in an exponential temperature dependence of the charge recombination rate, which was not observed. Rather, the result is consistent with a model in which the energy of both P^+I^- and P^+Q^- is uniformly shifted in the mutants (Fig. 4). Although the mutations may alter the reorganization energy, any such changes seem likely to be relatively small because the mutations are near the dimer and the major contribution to the reorganization energy is probably from the polar groups near the quinone. The relationship between the charge recombination rate and driving force has been studied previously by altering the driving force either by the application of electric fields or by replacing the native ubiquinone with quinones with other redox potentials (25–28). The estimates for the reorganization energy have varied from 500 to 970 meV; possible reasons for this large range, such as nonexponential kinetics and the use of multiple vibrational modes, have been discussed in detail elsewhere (27, 28).

An increase in the P/P^+ midpoint potential should decrease the driving force for the initial forward electron transfer reaction (Fig. 4), and a decrease in the rate of P* decay has been observed in several mutants that have an increase in the P/P^+ potential (5, 9, 29). Since the expected increase in the energy of the P^+I^- state by up to 260 meV is larger than the P^*/P^+I^- energy difference of 120–200 meV estimated from the P* fluorescence decay (reviewed in ref. 30), it is surprising that the forward electron transfer reaction can even occur in the mutants. However, the midpoint potentials derived from oxidation–reduction titrations are equilibrium measurements and thus pertain to fully relaxed systems, whereas measurements of the energy difference indicate that it evolves over the time of the initial electron transfer (30). In addition, this view assumes a conventional electron transfer mechanism, which may not be valid for the initial charge separation. Instead, the process has been modeled as being driven by the reorganization of the protein, which limits the rate of charge separation between strongly coupled cofactors (29).

Although the reaction centers are functional, the lower photosynthetic growth rates of the mutants indicate that energy conversion is not as efficient as in wild type. Several electron and energy transfer reactions in addition to the charge recombination and initial electron transfer may be affected by the change in the P/P^+ midpoint potential. An increase in the midpoint potential should increase the driving force for the reduction of P^+ by cytochrome c_2 and lead to a change in the rate of this reaction. Perhaps a more important factor is that an increase in the energy of P^+I^- could impair the ability of the reaction center to trap by charge separation the energy transferred from the antenna complexes. The lowered effective utilization of light energy would lead to slower photosynthetic growth in the mutants.

The largest change in midpoint potential due to a single mutation in the set of mutants described here was the increase of 125 mV observed in the FH(M197) mutant. A similarly large change in midpoint potential was observed for the analogous mutation in reaction centers from *Rb. capsulatus* (7, 8). In contrast, addition of a hydrogen bond to the dimer at the same position through mutation to a tyrosine residue at M197 results in a fairly small, 30-mV increase in the oxidation potential in *Rb. sphaeroides* (31). The larger change in oxidation potential for histidine could be due to differences in the strength of the hydrogen bond or in the chemical nature of the hydrogen donor (16). Most other types of reaction center mutations described previously change the midpoint potential of P by <60 mV compared with wild type (7, 31, 32). The only mutant with a comparable change, of 160 mV, is the "heterodimer" mutant (33). This mutant has a Bchl–bacteriopheophytin dimer that arises when one of the two histidine ligands to the Bchls is changed to leucine (34, 35). Associated with the change in cofactor composition are structural changes, including an $\approx$0.3-Å change in the posi-

tion of one of the dimer tetrapyrroles and up to 1.3-Å changes in the positions of aromatic residues near the dimer, compared with wild type (14). Although no direct structural information is available for the hydrogen-bond mutants, a variety of spectroscopic studies are consistent with well-defined, local changes of the structure due to the alteration of hydrogen bonding (5, 9, 10, 15, 16). The only exceptions appear to be reaction centers with the L168 mutation, in which the altered optical spectra suggest small changes in the structure of P.

Although metal coordination is a major influence on the redox properties of cofactors, other protein–cofactor interactions must play a role in determining the potentials, since a wide range of midpoint potentials are observed in biological systems that have identical coordination. Effects of interactions with nonligand residues on midpoint potentials have been demonstrated by site-directed mutations in cytochromes and in blue copper proteins, but most of these mutations result in small changes in potential that are not in any specific direction (reviewed in ref. 36). Compared with the effects of other nonligand mutations, the several-hundred-millivolt increases in potential observed in the histidine hydrogen-bond mutants are remarkable. These mutations demonstrate that successive increases in the midpoint potential of an electron donor can be attained by the addition of specific interactions of the donor with histidines that are not involved in metal coordination. This identifies a type of interaction that may contribute to the tuning of midpoint potentials of cofactors in other proteins.

A major difference between bacterial reaction centers and plant photosystem II is the ability of the plant reaction center to oxidize water. This function requires a very high oxidation potential (at least 1 V) for the primary electron donor, P680, in photosystem II. In this respect, these mutations make the bacterial reaction centers more similar to photosystem II. An additional 200-mV increase in the oxidation potential of P680 would be expected, since photosystem II contains chlorophyll *a*, which is inherently more difficult to oxidize than Bchl *a* (reviewed in ref. 37). These results demonstrate that protein–chlorophyll interactions can substantially contribute to the high potential of P680. The protein–chlorophyll interactions in photosystem II are unlikely to be exactly the same as those in bacterial reaction centers, especially in light of the low overall conservation of residues in the sequences of reaction centers from bacteria and plants (38). For example, no histidine residues are found in the photosystem II sequences at the positions homologous to those that form hydrogen bonds in the bacterial reaction center, and the proton-accepting carbonyl group on ring I is not present in chlorophyll *a*. Another important consequence of the difference in pigments in the two types of electron donors is that chlorophyll *a* absorbs light at higher energy than Bchl *a*, so that both the P/P^* transition and the P/P^+ potential are higher in photosystem II than in bacterial reaction centers. Thus the evolution from bacterial to plant reaction centers involved changes both in the pigment composition and in the pigment–protein interactions that modify the potential.

We thank V. H. Coryell, A. Juth, and A. K. W. Taguchi for assistance in the construction of the mutants. This work was supported by grants from the National Institutes of Health (GM45902) and the National Science Foundation (DMB-9111599 and MCB-9404925). This is publication no. 203 from the Arizona State University Center for the Study of Early Events in Photosynthesis.

1. Kirmaier, C. & Holten, D. (1987) *Photosynth. Res.* **13**, 225–260.
2. Feher, G., Allen, J. P., Okamura, M. Y. & Rees, D. C. (1989) *Nature (London)* **339**, 111–116.
3. Parson, W. W. (1991) in *Chlorophylls*, ed. Scheer, H. (CRC, Boca Raton, FL) pp. 1153–1180.
4. Moss, D. A., Leonhard, M., Bauscher, M. & Mäntele, W. (1991) *FEBS Lett.* **283**, 33–36.
5. Williams, J. C., Alden, R. G., Murchison, H. A., Peloquin, J. M., Woodbury, N. W. & Allen, J. P. (1992) *Biochemistry* **31**, 11029–11037.
6. Nagarajan, V., Parson, W. W., Davis, D. & Schenck, C. C. (1993) *Biochemistry* **32**, 12324–12336.
7. Taguchi, A. K. W., Stocker, J. W., Alden, R. G., Causgrove, T. P., Peloquin, J. M., Boxer, S. G. & Woodbury, N. W. (1992) *Biochemistry* **31**, 10345–10355.
8. Stocker, J. W., Taguchi, A. K. W., Murchison, H. A., Woodbury, N. W. & Boxer, S. G. (1992) *Biochemistry* **31**, 10356–10362.
9. Williams, J. C., Alden, R. G., Coryell, V. H., Lin, X., Murchison, H. A., Peloquin, J. M., Woodbury, N. W. & Allen, J. P. (1992) in *Research in Photosynthesis*, ed. Murata, N. (Kluwer, Dordrecht, The Netherlands), Vol. 1, pp. 377–380.
10. Murchison, H. A., Alden, R. G., Allen, J. P., Peloquin, J. M., Taguchi, A. K. W., Woodbury, N. W. & Williams, J. C. (1993) *Biochemistry* **32**, 3498–3505.
11. Yeates, T. O., Komiya, H., Chirino, A., Rees, D. C., Allen, J. P. & Feher, G. (1988) *Proc. Natl. Acad. Sci. USA* **85**, 7993–7997.
12. Chang, C.-H., El-Kabbani, O., Tiede, D., Norris, J. & Schiffer, M. (1991) *Biochemistry* **30**, 5352–5360.
13. Mattioli, T. A., Hoffmann, A., Robert, B., Schrader, B. & Lutz, M. (1991) *Biochemistry* **30**, 4648–4654.
14. Chirino, A. J., Lous, E. J., Huber, M., Allen, J. P., Schenck, C. C., Paddock, M. L., Feher, G. & Rees, D. C. (1994) *Biochemistry* **33**, 4584–4593.
15. Nabedryk, E., Allen, J. P., Taguchi, A. K. W., Williams, J. C., Woodbury, N. W. & Breton, J. (1993) *Biochemistry* **32**, 13879–13885.
16. Mattioli, T. A., Williams, J. C., Allen, J. P. & Robert, B. (1994) *Biochemistry* **33**, 1636–1643.
17. Paddock, M. L., Rongey, S. H., Feher, G. & Okamura, M. Y. (1989) *Proc. Natl. Acad. Sci. USA* **86**, 6602–6606.
18. Kleinherenbrink, F. A. M., Chiou, H. C., LoBrutto, R. & Blankenship, R. E. (1994) *Photosynth. Res.* **41**, 115–123.
19. Wells, J. A. (1990) *Biochemistry* **29**, 8509–8517.
20. Rautter, J., Gessner, C., Lendzian, F., Lubitz, W., Williams, J. C., Murchison, H. A., Wang, S., Woodbury, N. W. & Allen, J. P. (1992) in *The Photosynthetic Bacterial Reaction Center: Structure, Spectroscopy, and Dynamics*, eds. Breton, J. & Verméglio, A. (Plenum, New York), Vol. 2, pp. 99–108.
21. Marcus, R. A. & Sutin, N. (1985) *Biochim. Biophys. Acta* **811**, 265–322.
22. Jortner, J. (1976) *J. Chem. Phys.* **64**, 4860–4867.
23. Arata, H. & Parson, W. W. (1981) *Biochim. Biophys. Acta* **638**, 201–209.
24. Kleinfeld, D., Okamura, M. Y. & Feher, G. (1984) *Biochim. Biophys. Acta* **766**, 126–140.
25. Gunner, M. R. & Dutton, P. L. (1989) *J. Am. Chem. Soc.* **111**, 3400–3412.
26. Popovic, Z. D., Kovacs, G. J., Vincett, P. S., Alegria, G. & Dutton, P. L. (1986) *Chem. Phys.* **110**, 227–237.
27. Feher, G., Arno, T. R. & Okamura, M. Y. (1988) in *The Photosynthetic Bacterial Reaction Center*, eds. Breton, J. & Verméglio, A. (Plenum, New York), pp. 271–287.
28. Franzen, S. & Boxer, S. G. (1993) *J. Phys. Chem.* **97**, 6304–6318.
29. Woodbury, N. W., Peloquin, J. M., Alden, R. G., Lin, X., Lin, S., Taguchi, A. K. W., Williams, J. C. & Allen, J. P. (1994) *Biochemistry* **33**, 8101–8112.
30. Peloquin, J. M., Williams, J. C., Lin, X., Alden, R. G., Taguchi, A. K. W., Allen, J. P. & Woodbury, N. W. (1994) *Biochemistry* **33**, 8089–8100.
31. Wachtveitl, J., Farchaus, J. W., Das, R., Lutz, M., Robert, B. & Mattioli, T. A. (1993) *Biochemistry* **32**, 12875–12886.
32. Jia, Y., DiMagno, T. J., Chan, C.-K., Wang, Z., Du, M., Hanson, D. K., Schiffer, M., Norris, J. R., Fleming, G. R. & Popov, M. S. (1993) *J. Phys. Chem.* **97**, 13180–13191.
33. Davis, D., Dong, A., Caughey, W. S. & Schenck, C. C. (1992) *Biophys. J.* **61**, 153 (abstr.).
34. Bylina, E. J. & Youvan, D. C. (1988) *Proc. Natl. Acad. Sci. USA* **85**, 7226–7230.
35. McDowell, L. M., Gaul, D., Kirmaier, C., Holten, D. & Schenck, C. C. (1991) *Biochemistry* **30**, 8315–8322.
36. Wuttke, D. S. & Gray, H. B. (1993) *Curr. Opin. Struct. Biol.* **3**, 555–563.
37. Watanabe, T. & Kobayashi, M. (1991) in *Chlorophylls*, ed. Scheer, H. (CRC, Boca Raton, FL), pp. 287–315.
38. Komiya, H., Yeates, T. O., Rees, D. C., Allen, J. P. & Feher, G. (1988) *Proc. Natl. Acad. Sci. USA* **85**, 9012–9016.